USE OF CFD FOR THE DESIGN OF INJECTORS FOR SUPERCRITICAL WATER OXIDATION

J.P. Serin[(1)], J. Mercadier[(1)], F. Marias*[(1)], P. Cezac[(1)], F. Cansell[(2)]
(1) Laboratoire Thermique Energétique et Procédés (EA 1932), ENSGTI
Rue Jules Ferry, B.P. 7511, 64075 Pau Cedex, France
Tel : +33 (0) 559 407 800, Fax : +33 (0) 559 407 801,
(2) Institut de Chimie de la Matière Condensée de Bordeaux
87 avenue du Docteur Albert Schweitzer, 33608 Pessac Cedex, France

ABSTRACT

This paper focuses on the design of oxygen injectors for supercritical water oxidation processes. More precisely, in the case of multi injection tubular reactor, it is necessary to ensure rapid and efficient mixing of oxygen and aqueous waste in order to obtain higher conversion of the organic content. Because such reactors operate at high pressure (25MPa) and high temperature (700K) it is difficult to make experiments to design such devices. Thus, in this study, Computational Fluid Dynamics has been used in order to obtain information on the efficiency of 5 different configurations. The analysis of the results has shown that for safety reasons, some of these configurations should be prohibited. Finally, it has given determinant information for the final decision making process of the geometry of the injector.

INTRODUCTION

Hydrothermal oxidation of aqueous wastes under supercritical conditions is a well known process [1],[2],[3], [4]. It is typically able to treat concentrations of organic waste from 1 to 10%. The basic principle of this treatment is to oxidise organic matter into carbon dioxide and water, and inorganic material into mineral salts, using a supercritical fluid as the reacting media. Aqueous waste is pumped from a storage raised to 25MPa and preheated to approximately 673K. It is then supplied to a chemical reactor where it is mixed with oxygen in order to be converted to carbon dioxide and water. The mixture leaving the reactor is cooled before entering a back pressure valve where pressure is dropped. The expended fluid then enters a flash where gaseous and liquid components are separated.

At present time, a lot of reactor geometry exists, both at industrial and pilot scale [5], [6]. This paper focuses on the tubular reactor. In such geometry, on of the key parameter is how to inject oxidant in order to run the process in the “safe mode” [6]. Conceptually, Cansell [7] have shown that a multi-injection reactor kept the inside temperature at smaller values and prevented reactor runaways. This geometry is thus very attractive, but, the question that remains is how to design these injectors. Indeed, this design must fulfil the two following requirements:

- allow rapid and good mixing between oxidant and mixture,
- avoid high concentration of oxygen near the walls of the reactor that would lead to rapid corrosion at this pressure and temperature.

This study focuses on the design of theses injectors. More precisely, in this paper CFD (Computational fluids dynamics) is used in order to compare 5 different geometries and to check for their respective efficiencies.

In a first part, the system under study will be presented. Features of the reactor (in terms of diameter, flow rates, operating conditions) are shown as well as the 5 injectors geometries that we have chosen to focus on. Also, in this part, are discussed the thermodynamics and transport properties of the mixture.

The second part of the paper is devoted to the computational part itself. Models used in the CFD package are given and the simulation results are presented.

I - SYSTEM UNDER STUDY

I.1 - Features of the reactor

The reactor under study is designed to process 1t/h of aqueous waste with a maximum of 5% of organic content on a weight basis. Its internal diameter is 2.54 cm (1'') while its length is approximately 100m. It is coiled shaped in order to reduce its size. The aqueous waste is supplied to the reactor at 673K. Three oxygen injectors have been disposed on the reactor in order to obtain the desired temperature profile [8]. The internal diameter of the oxygen pipe is 0.2381cm (3/32''). The oxygen is supplied to the reactor at 300K. Both fluids enter the reactor at 25MPa. In order to carry out the simulations, the aqueous waste has been supposed to be composed of 4% of phenol (on a weight basis). Given the mass flow rate of aqueous waste, the stoechiometric quantity of oxygen required for the conversion of phenol is 95.32kg/h. Thus, we assume that the mass flow rate of oxygen supplied to each injector is 32kg/h.

I.2 - Physical properties of fluids

Because of its low organic content, the aqueous waste is supposed to behave as pure water. Thus, density, heat capacity, thermal conductivity and viscosity of the aqueous waste are computed from the IAPWS formulation for pure water [9]. The computation of oxygen properties has been performed using Pitzer's method [10]. The results show much more regular trends than in the case of pure water because we are far above the critical point of pure oxygen (154.4K, 5.04MPa).

Thus, above 673K, the two fluids in question are above their critical points. That is why, the mixing results we are interested in, are only relative to homogenous mixing. There is no dissolution or boiling phenomenon. Moreover, because oxygen is a non polar molecule, and because above its critical point, water is known to have a very small dielectric constant [5], we expect that the mixture between water and oxygen is ideal. Thus the properties of the mixture water oxygen are computed from the properties of the pure fluids balanced by their mass fraction inside the mixture.

I.3 - Geometry of the injectors

It has been quoted previously that the diameter of the supplies of oxygen is 0.2381 cm (3/32'') while the diameter of the reactor is 2.54 cm (1''). The choice of this size has been done in order to have velocity of the same order of magnitude both in the reactor and in the supplies of oxygen. More precisely, for a mass flow-rate of waste of 1 t/h entering the reactor at 673 K and 25 MPa, its superficial velocity is approximately $3 m.s^{-1}$, while, for the oxygen entering the injector, it is approximately $6 m.s^{-1}$. Moreover, five geometries have been tested, two of the collinear type (upper collinear, central collinear) and three of the transversal type (90°, 180°, and, 45°). On Figure 1, a sketch of the five injectors is given.

II - SIMULATIONS AND RESULTS

The CFD package Fluent™ [11] has been used in order to compute the flow-fields of oxygen mass fraction, velocity, density and temperature inside the reactor. In this part, we give insights on the simulated domain, the scheme used for its meshing and the models we have used in order to carry out the simulations. Then, we present the results obtained after simulations. Profiles of mass fraction of oxygen downstream the injections are compared and inspection of the different quoted fields give information on which injector to choose.

II.1 - Domain, meshing, models and boundary conditions

Computational domain

The length of the reactor is approximately 100 m while its diameter is only 2.54cm. It would be a non-sense to simulate the whole reactor because we are only interested in the vicinity of

the injector. That is why some preliminary computations have been carried out in order to check where we should end the domain under study. These computations have shown that for any of the five configurations under study, a length of 1.5m was sufficient. We mean that, in every case, mixing between oxygen and waste was complete 1.5m downstream the injector. That is why this length has been fixed as the limit of our computational domain. Of course, the domain under study is fully three dimensional. Nevertheless, a 3D simulation would not give much more information than a 2D one as long as all of the boundary conditions are of the axysymetric type, except at the supply of oxygen. Moreover, 3D simulations require much more memory and CPU capacities. Thus, the choice has been made to perform 2D simulations, on a longitudinal cut of the reactor.

Meshing

Fluent™ uses finite volume [12] as discretization scheme, in order to convert partial differential equation into algebraic ones. Thus the meshing of the domain is required. In our case, we have chosen a meshing algorithm that separates the domain under study into triangles on which balances are performed. Figure 2 illustrates such a discretization. Of course, the number of these control volumes (cells) can drastically modify the results of the simulations. Indeed, a non sufficient number of cells would lead to inaccurate results. In our case, we have performed simulations on coarse mesh and then refine them until the results are independent of the number of cells. Table 1 give information on the total number of nodes that have been used in this work.

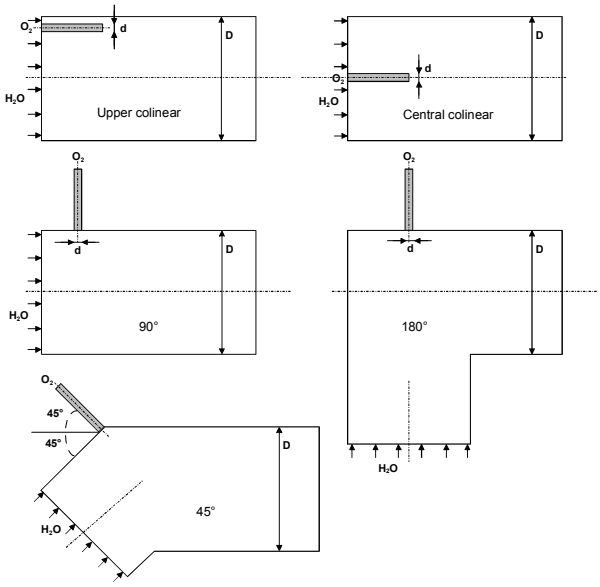

Figure 1: Sketch of the geometry of the injectors under consideration

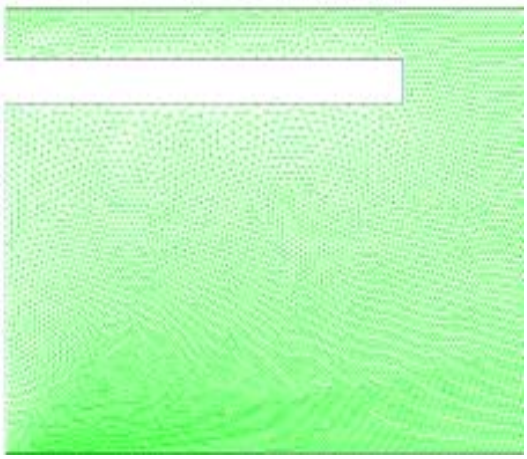

Figure 2: Detail of the mesh near the supply of oxygen for the upper collinear injector

Table 1: Number of cells used for meshing and Reynolds's number at inputs

	Collinear		Transversal		
	Upper collinear	Central collinear	90°	180°	45°
Total number of cells	80 310	76 736	90 630	106 410	102 802
Reynolds number (waste)	469 890	469 890	465 190	465 190	465 190
Reynolds's number (oxygen)	214 830	214 830	214 830	214 830	214 830

Models

Basically, the equations that are solved in the software Fluent™, are mass, species, momentum and energy balances [11]. As it shown into Table 1, the flow is fully turbulent inside the reactor. In order to take into account this particular phenomenon, all of the state variables are expressed as a sum of an average value and a fluctuation (Reynolds' averaging):

$$\phi = \overline{\phi} + \phi' \tag{1}$$

Inserting this sum into the momentum balance for velocities, one is able to reveal the Reynolds' tensor: $-\rho\overline{u_i' u_j'}$. Also, inserting such sum into species and enthalpy balances, one is able to reveal other average of product fluctuations. Using the Boussinesq's assumption [13], these products are expressed as the product of a turbulent transport property, multiplied by the gradient of the appropriate average quantity. This is very similar to the definition of mass diffusivity, thermal conductivity and dynamic viscosity using the Fick's first law, Fourier's law and Newton's law for molecular transport of species, energy and momentum respectively. The quoted products are expressed as:

$$-\rho\overline{u_i' u_j'} = \mu_t\left(\frac{\partial \overline{u_i}}{\partial x_j} + \frac{\partial \overline{u_j}}{\partial x_i}\right) \tag{2}$$

$$-\rho\overline{u_i' y_k'} = \rho D_{kt}\frac{\partial \overline{y_k}}{\partial x_i} = \frac{\mu_t}{Sc_t}\frac{\partial \overline{y_k}}{\partial x_i} \tag{3}$$

$$-\rho\overline{u_i' h'} = \lambda_t\frac{\partial \overline{T}}{\partial x_i} = \frac{c_p\mu_t}{\mathrm{Pr}_t}\frac{\partial \overline{T}}{\partial x_i} \tag{4}$$

The computation of the turbulent viscosity is performed using the k-ε model [14] (Marias *& al*. [15] have shown that the information provided by this model for non swirling jet analysis). Basically, using this model, a transport equation is solved for the kinetic energy of turbulence and its dissipation. The turbulent viscosity is then computed following the relation

$$\mu_t = \rho C_\mu\frac{k^2}{\varepsilon} \tag{5}$$

The turbulent Schmidt's and Prandtl's numbers are supposed to be constant over the computational domain. The different equations solved by the software using the standard k-ε model are available in the user's guide [11]. Using the finite volume method for discretization, one also needs to specify interpolation schemes. The default schemes of the software have been kept.

To conclude with the models, we have to add that the physical properties of the fluids and the mixture of fluids have been computed outside the software using User Defined Functions written in C language. Such functions have been defined for density, thermal conductivity, and viscosity. In the case of heat capacity of fluids, they have been input into the software through piecewise linear functions.

Table 2: Boundary conditions used

	Collinear				Transversal					
	Upper collinear		Central collinear		90°		180°		45°	
	Waste	O_2	Waste	O_2	Waste	O_2	Waste	O_2	Waste	O_2
Velocity magnitude ($m.s^{-1}$)	3.12	5.25	3.12	5.25	3.09	5.25	3.09	5.25	3.09	5.25
Temperature (K)	673	300	673	300	673	300	673	300	673	300
Intensity of turbulence (%)	10	10	10	10	10	10	10	10	10	10

Characteristic length scale of turbulence (m)	0.025	0.002	0.025	0.002	0.025	0.002	0.025	0.002	0.025	0.002
Mass fraction of O_2 (-)	0	1	0	1	0	1	0	1	0	1

Boundary conditions

In terms of boundary conditions, 5 quantities are required at input conditions. They are: velocity magnitude (and its direction) temperature, intensity of turbulence and characteristic length of turbulence. Also, the mass fraction of oxygen is required at each input. Table 2 summarises these conditions at the waste input and at the oxygen supply. Dealing with the wall lining the domain, the only one condition required is relative to the heat flux across the wall. Because the reactor is sufficiently insulated, we have assumed that these walls were adiabatic.

II.2 - Results

This section presents the results of the computation after convergence of the software. Convergence is checked using the default criteria of the commercial code.

Figure 3 represents the profile of mass fraction of oxygen at different locations downstream the injector. These locations are *1d*, *5d*, *10d*, *50d*, *100d*, *200d* and *500d*, where *d* denotes the diameter of the oxygen supply (0.0024m). Figure 4a and 4b shows fields of mass fraction of water, temperature density and velocity vectors in the vicinity of the injection point.

The first point to mention is the difference of density between the two input streams. Whereas aqueous waste enters the injection region at 673K, the O_2 is supplied at 300K. The corresponding values for density are respectively 200 and 373 $kg.m^{-3}$. One could expect that this difference would lead to buoyancy effects that would enhance mixing. This is the reason why on every studied case, the supply of oxygen had been located on the upper part of the injector. The inspection of the velocity vectors on Figures 4 reveals that these gravity effects seem to direct the oxygen stream towards the bottom of the injector. Nevertheless, the inspection of these figures also shows that, the region of lower temperature linked to oxygen injection is very narrow, especially in the case of collinear injections. The high value of the specific heat of pure water at 673K ($\approx$ 13 000 $J.kg^{-1}.K^{-1}$), associated with a high mass flow rate of waste compared to the oxygen one, lead to a rapid homogenisation of the temperature in the vicinity of the injection. Thus, on a short distance after the oxygen supply, the density difference linked to temperature gradients becomes negligible and thus the buoyancy effects vanish. This phenomenon is also confirmed by the examination of the fields of density on the quoted figures.

Still regarding these figures, one can remark that in the case of the transversal injectors, there exists a zone near the supply of oxygen where the temperature is kept to a low value. The problem is that this region is located near the wall of the reactor and it can lead to high gradients inside the reactor material. Keeping in mind that the operating pressure is high (25MPa), such gradients must be prohibited in order to enhance the resistance of the reactor material. Transversal injectors do not seem to fulfil the requirements of safety of the reactor.

Such a conclusion can also be drawn regarding the fields of water mass fraction. Indeed, blue colour indicates high value of oxygen, whereas red indicates high value of water. The point is that all of the transversal injectors have high oxygen content at the wall of the reactor. Once again, such a situation is prohibitive because it might lead to corrosion and to an unsafe mode of operation of the reactor. This is particular the case for the “45°” injector where these regions of high oxygen concentration and low temperature are the largest.

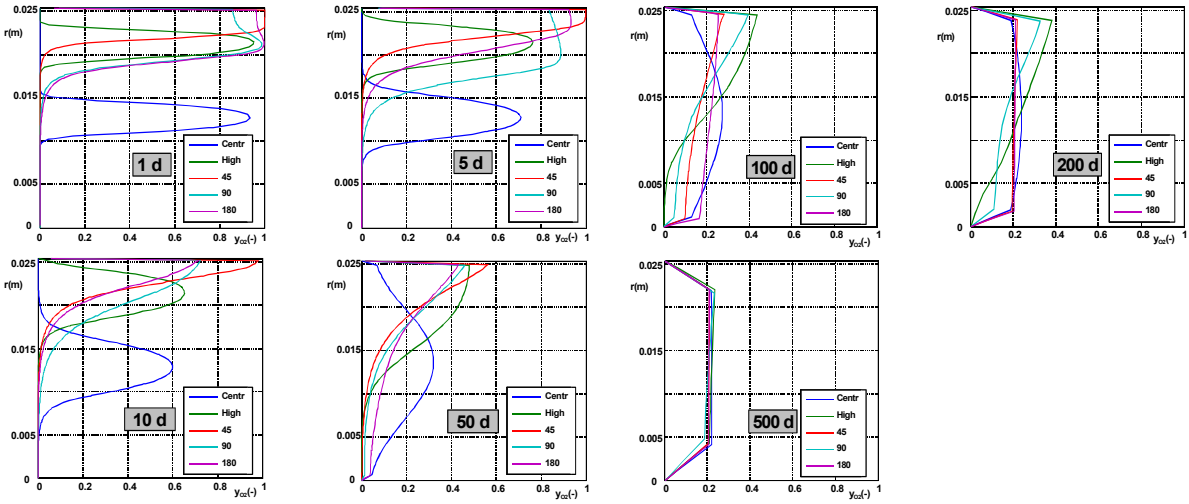

Figure 3: Profile of mass fraction of oxygen downstream the injector

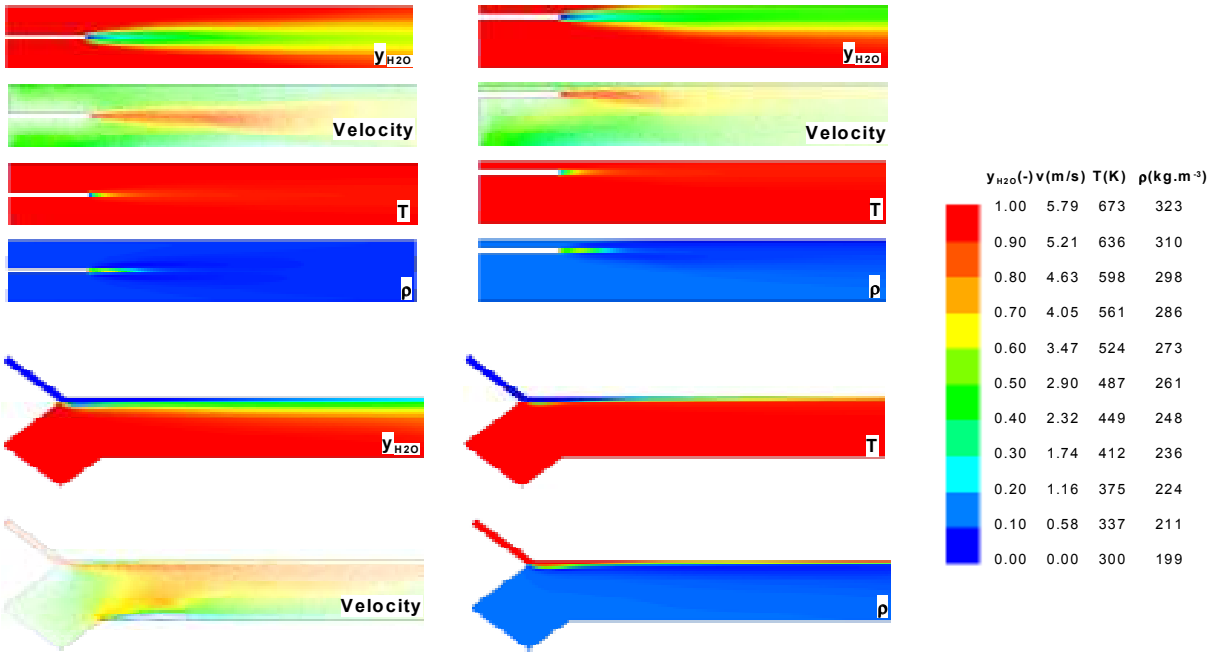

Figure 4a: Fields of oxygen mass fraction, velocity vectors, temperature and density for the different injectors

Dealing with the efficiency of the devices under consideration, Figure 3 shows that before 50d (≈ 10 cm) no mixing has been really performed yet. Indeed, below this location, we still remark the high concentration of oxygen on the near wall region, and also one can see that only low dispersion of the oxygen stream has been performed. 50d after the supply of oxygen, only the "180°" and "central collinear" injector seem to have ensured mixing of fluids. This conclusion is also valid 100d (≈20 cm) and 200d (≈ 40cm) downstream the injection device. The "45°" is also efficient at this distance from the oxygen supply.

Regarding the whole set of information given by the results of simulation, we can say that the in terms of efficiency, the better injectors are the "central collinear", the "180°" and the "45°". Nevertheless, the two last of the quoted injectors have shown problems that might attempt to the safety of the reactor. Thus, the device we have chosen for operation is the central collinear one.

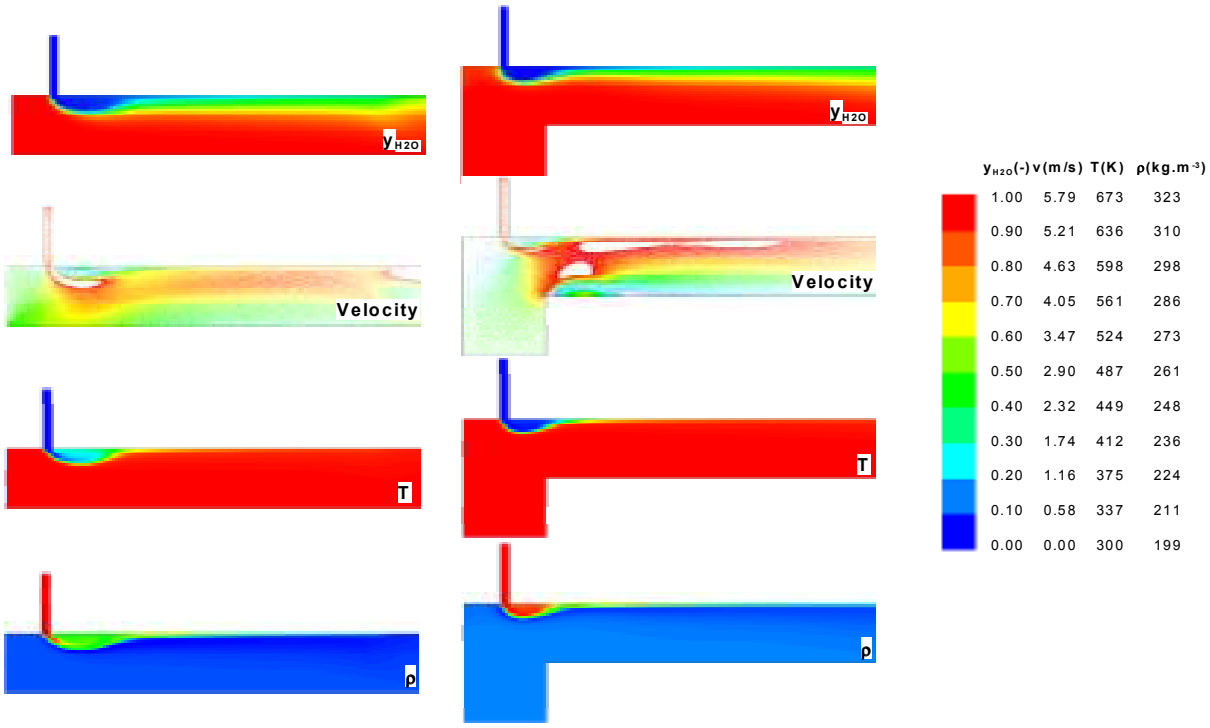

Figure 4b: Fields of oxygen mass fraction, velocity vectors, temperature and density for the different injectors (continued)

CONCLUSION

This paper has presented the methodology that we have used in order to design devices for the injection of supercritical oxygen into supercritical aqueous waste for reduction of organic content. The hard conditions (in terms of pressure and temperature) that prevail into such process do not allow designing such devices by conventional methods (experimental setup, measure and analysis). Thus, Computational Fluid Dynamics has been used in order to obtain information on the efficiency of 5 devices under study. Basically, a CFD software allows for the simultaneous solving of mass, species, momentum and energy equations in turbulent conditions on a given geometry. As a result, given a configuration (models, physical properties, boundary conditions), it yields cartographies of velocity temperature and species mass fraction. In our case, once the computational domain has been fixed, one of the issues we have to address was the dependence of the physical properties of fluids on both temperature and composition. This problem has been solved using external routines in C language that allow for the computation of the physical properties of the mixture.

The examination of the results has shown that some configuration could lead to rapid degradation of the safety of the reactor. Indeed there is evidence that these configurations would lead to high thermal gradients inside the material of the reactor associated with high oxygen concentration in the vicinity of the wall, that would in turn, lead to corrosion of the reactor. It has also shown differences in the efficiency (in terms of quality of mixing) of the devices under study. This study has revealed that we should design the injector as “central collinear”, because, this geometry is one of the most efficient, and it is not linked to thermal gradients or high oxygen concentration near the wall of the reactor.

ACKNOWLEDGEMENTS

We wish to thank the French minister of economy and the European Union (Interreg IIIb, Atlantic area) for his financial support to this work.

REFERENCES

[1] DUTOURNIE, P., PhD Thesis, Université de Pau et des Pays de l'Adour 2000.

[2] CANSELL F., REY S., BESLIN P., Revue de l'Institut Français du Pétrole, Vol. 53, **1998**, p. 71

[3] CANSELL F., BESLIN P., BERDEU B., Environmental Progress, Vol 17, **1998**, p. 240

[4] TESTER J. W., HOLGATE H. R., AMELLINI F. J., WEBLEY P. A., KILLILEA W. R., HONG G. T., BARNER H. E., ACS Symp. Ser., vol. 518, **1993**, p. 35

[5] MERCADIER J., VIELCAZALS S., Supercritical fluids and materials, ed. N. BONNAUDIN, F. CANSELL and O. FOUASSIER. Biarritz: Institut national polytechnique de lorraine, ISBN 2-905267-39-9, **2003**, p. 277

[6] BOTTREAU M., *Supercritical fluids and materials*. Supercritical fluids and materials, ed. N. BONNAUDIN, F. CANSELL, and O. FOUASSIER. Biarritz: Institut national polytechnique de lorraine, ISBN 2-905267-39-9, **2003**, p. 369

[7] CANSELL F., CNRS Patent - WO 0220414

[8] Hydrothermale Oxydation Option (HOO), http://www.hoo-ingenierie.fr/

[9] WAGNER W., KRUSE A., The Industrial Standard IAPWS-IF97 for the Thermodynamic Properties and Supplementary Equations for other Properties, Properties of Water and Steam, Springer, **1998**

[10] REID R.C., PRAUSNITZ J.M., SHERWOOD T.K., The properties of gases and liquids, Third Edition, McGraw-Hill, **1977**

[11] Fluent User's guide

[12] PATANKAR S.V., Numerical Heat Transfer and Fluid Flow**,** Hemisphere Publishing Corporation, Washington, DC, **1980**

[13] BOUSSINESQ J., Théorie de l'écoulement tourbillonnant, Mémoire présenté par la division savante. Paris, **1877**

[14] LAUNDER B.E., SPALDING D.B., Mathematical Models of Turbulence, Academic Press, London, **1972**

[15] MARIAS F., PUIGGALI J.R., QUINTARD M., PIT F., The Korean Journal of Chemical Engineering, Vol 19, **2002**, p. 28